Enhancing Functional Neuroimages

Wink, Alle Meije; Roerdink, Jos B.T.M.

Published in:
EPRINTS-BOOK-TITLE

Publication date:
2002

Alle Meije Wink[1]**, Jos B.T.M. Roerdink**[2]

[1,2] Institute for Mathematics and Computing Science
   and
   Institute for Behavioral and Cognitive Neurosciences,
   University of Groningen,The Netherlands
[1] `wink@cs.rug.nl`
[2] `roe@cs.rug.nl`

ENHANCING FUNCTIONAL NEUROIMAGES: WAVELET DENOISING AS AN ALTERNATIVE TO GAUSSIAN SMOOTHING

Abstract

We present a general wavelet-based denoising scheme for functional neuroimages and compare it to Gaussian smoothing, the standard method in functional neuroimaging. We adapted WaveLab thresholding routines to 2D data, and tested their effect on the signal-to-noise ratio of noisy images. In a simulated time series test, we also investigated the shapes of detected activations after denoising.

   keywords: *Wavelets, functional neuroimaging, denoising, signal-to-noise ratio*

1   INTRODUCTION

Functional neuroimages are often denoised by convolving them with a Gaussian smoothing kernel. This removes noise but it also changes the intensity variation of the underlying image; details in the image are suppressed. We propose wavelet denoising as an alternative to Gaussian smoothing.

We focus on functional magnetic resonance imaging (fMRI) time series. In an fMRI experiment, a series of scans is made of a test person performing a task inside an MRI scanner. Local magnetic properties change in brain regions involved in that task, due to local changes in blood oxygenation levels [1]. Detecting and describing those changes is the key task in fMRI time series analysis. Statistical analysis of fMRI data has already been done in the wavelet domain [2, 3] and in the spatial domain after denoising in the wavelet domain [4].

The novelty of this paper is the comparison of wavelet denoising and Gaussian smoothing, the standard denoising tool in functional neuroimaging. Wavelet thresholding was done with WaveLab routines [5], which were extended to 2D data. We tested these methods on images with known signal-to-noise ratios (SNRs) and noise distributions, and we investigated the SNRs after denoising. We also compared the shapes of detected regions in simulated time series with the original active region. Generally, wavelet-based methods introduce fewer detection errors because shapes in the images are less deformed.

The rest of this paper is organised as follows. In section 2, wavelet-based denoising is introduced. These schemes are tested on 2D images in section 3, and on a simulated fMRI time series in section 4. Section 5 contains some general conclusions.

2 WAVELET-BASED DENOISING

Wavelet bases are bases of nested function spaces, which can be used to analyse signals at multiple scales. Wavelet coefficients carry both time and frequency information, as the basis functions vary in position and scale. The fast wavelet transform (FWT) efficiently converts a signal to its wavelet representation [6]. Spline wavelet bases (see Fig. 1a) are well suited for image processing [7]. In a one-level FWT, a signal c_0 is split into an approximation part c_1 and
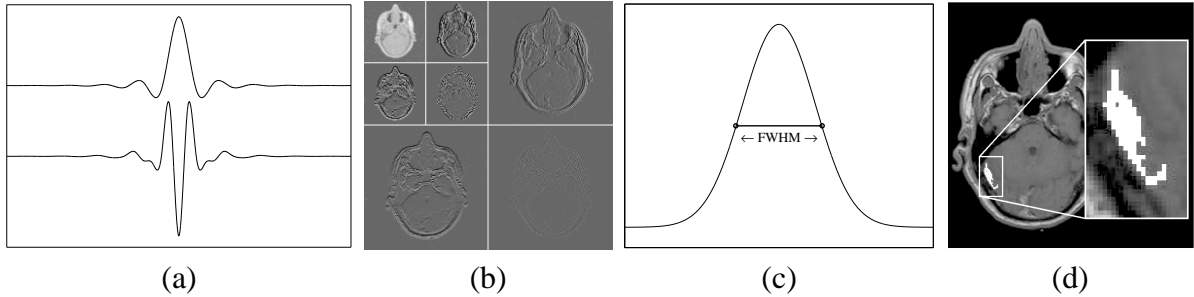
Figure 1. (a) Symmetric orthonormal cubic spline scaling function and wavelet, (b) a 2D wavelet transform of an MR image, (c) the full width at half maximum of a Gaussian, (d) the active spot in the simulated time series.

a detail part d_1. In a multilevel FWT, each subsequent c_i is split into an approximation c_{i+1} and detail d_{i+1}. For 2D images, each c_i is split into an approximation c_{i+1} and three detail channels d_{i+1}^1, d_{i+1}^2, and d_{i+1}^3, for horizontally, vertically, and diagonally oriented details, respectively (see Fig. 1b). The inverse FWT (IFWT) reconstructs each c_i from c_{i+1} and d_{i+1}.

The WaveLab package by Donoho et al. [5] contains thresholding schemes for wavelet-based denoising: InvShrink, MinMaxThresh, MultiMAD, SUREThresh, VisuThresh with hard or soft thresholding, HybridThresh, and WaveJS (James-Stein) [8, 9]. An important property of these denoising schemes is the degree of smoothness of the denoised image [4].

Wavelet denoising thresholds the detail coefficients. Determining the threshold for each decomposition level and each channel gives extra flexibility. Furthermore, with an unknown noise model, a level-dependent threshold is preferable. Therefore, our denoising routines process each detail channel at each scale (see Fig. 1b) individually. Orthogonal spline FWTs can be computed efficiently in the frequency domain [7]. This computation produces complex numbers, which cannot be thresholded directly because complex numbers are not ordered. We use the polar representation and threshold only the magnitudes, keeping the phases.

3 DENOISING 2D IMAGES

As a test, we used the wavelet-based and Gaussian denoising routines to enhance a 2D MR image. We used various degrees of Gaussian smoothing (characterised by the filter width, or FWHM, see Fig. 1c). The signal-to-noise ratio (SNR) of the images before and after denoising were compared as follows. We used white noise and $1/f$ noise for the tests. Noise $\epsilon_1(\boldsymbol{x})$ was added to the original image $f_0(\boldsymbol{x})$, yielding $f_1(\boldsymbol{x}) = f_0(\boldsymbol{x}) + \epsilon_1(\boldsymbol{x})$. Let σ_f denote the standard deviation of a signal f. The SNR of the noisy image was computed as $\mathrm{SNR}_1 = 10 \log_{10}(\sigma_{f_0}/\sigma_{\epsilon_1})$. The noise of the denoised image f_2 was computed as $\epsilon_2(\boldsymbol{x}) = f_2(\boldsymbol{x}) - f_0(\boldsymbol{x})$. This resulted in a new SNR, denoted by $\mathrm{SNR}_2 = 10 \log_{10}(\sigma_{f_0}/\sigma_{\epsilon_2})$.

white noise, Gaussian smoothing

white noise, wavelet denoising

$1/f$ noise, Gaussian smoothing

$1/f$ noise, wavelet denoising
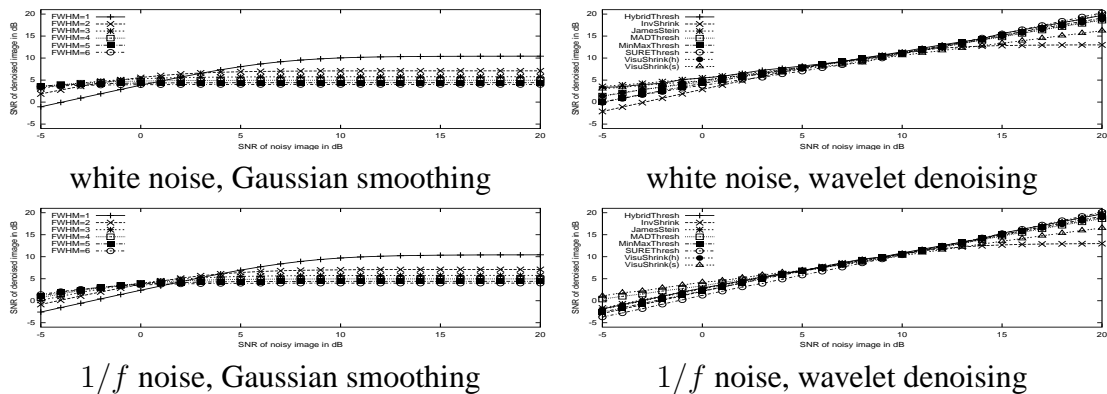
Figure 2. Performance of the denoising schemes. The SNR of the denoised image is plotted against the SNR of the noisy input image.

Fig. 2 shows SNR_2 plotted against SNR_1 for every tested method. Wider Gaussian smoothing kernels perform better for only the lowest input SNRs, and smaller kernels perform better with moderate and high input SNRs. All Gaussian smoothing methods have a maximum output SNR; this maximum decreases as the FWHM increases. The wavelet methods perform as well

as Gaussian smoothing for low SNRs, and better for higher SNRs. VisuThresh with soft thresholding is good for low SNRs, but not for high SNRs. SUREThresh performs badly for the lowest SNRs, but it is the best method for high SNRs. The difference between these methods is that VisuThresh with soft thresholding introduces relatively much smoothness in the images, while SUREThresh introduces little smoothness (see also [4]).

The output SNR of smoothing wavelet methods (HybridThresh, WaveJS, and VisuThresh with soft thresholding) are higher for low input SNRs, but as the input SNR increases, the output quality of the less smoothing wavelet methods improves faster. We discuss the effect of smoothing on shapes and intensity distributions in the images in greater detail in section 4. Wavelet denoising schemes perform consistently for both noise models we used, while the SNR improvement of Gaussian smoothing differs between white noise and $1/f$ noise. This is important, because for neuroimages the appropriate noise model is often unknown. To improve the SNR, wavelet denoising schemes provide a good alternative to Gaussian smoothing.

4   DENOISING A SIMULATED TIME SERIES

In most neuroimaging applications the SNR cannot be computed, because it is unknown which part of the signal is noise. Therefore, we constructed an artificial time series by making 64 copies of the MR image of the previous section, superimposing a time signal $b(t)$ on a small part of the image (see Fig. 1d), and adding noise with a known distribution and SNR. Let $\mathcal{F}_0^x(t)$ denote
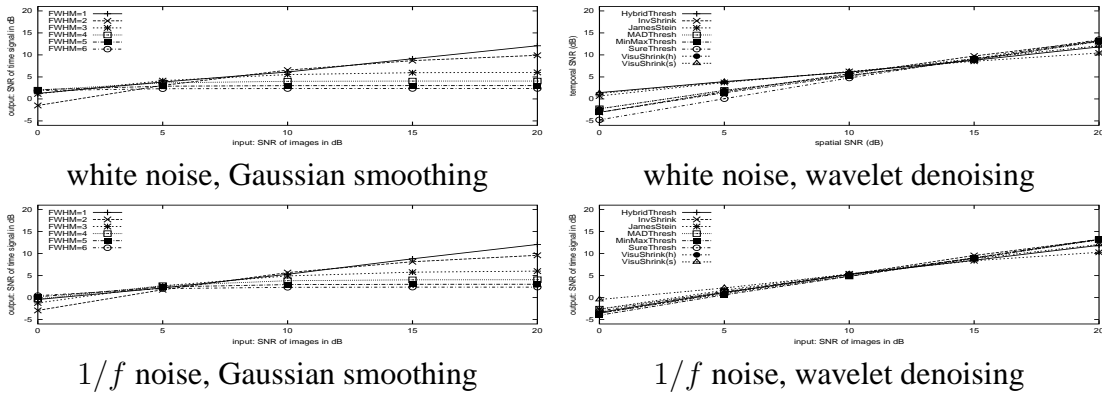

white noise, Gaussian smoothing   white noise, wavelet denoising

$1/f$ noise, Gaussian smoothing $1/f$ noise, wavelet denoising

Figure 3. Average of the temporal SNR_2^x over all voxels x of the original spot in the denoised time series, plotted against the input spatial SNR.

the value at position x and at time t of the time series with the time signal superimposed, but without noise, and $\mathcal{F}_1^x(t)$ and $\mathcal{F}_2^x(t)$ the noisy and denoised time series. The temporal noise and the temporal SNR are denoted by $\epsilon_2^x(t) = \mathcal{F}_2^x(t) - \mathcal{F}_0^x(t) - b(t)$ and $\text{SNR}_2^x = 10 \log_{10}(\sigma_b/\sigma_{\epsilon_2^x})$, where σ_b and $\sigma_{\epsilon_2^x}$ are the temporal standard deviations of $b(t)$ and $\epsilon_2^x(t)$, respectively.

4.1 Effect on the temporal SNR

Fig. 4 shows the average of SNR_2^x over all voxels x inside the active spot, as a function of the spatial input SNR. Gaussian smoothing with a larger FWHM performs better for a low input spatial SNR, but this hardly improves when the input SNR increases. For higher input SNRs, smaller kernels are better, because they deform the image less severely. The wavelet-based methods generally perform better than Gaussian smoothing, except for low SNRs. Smoothing wavelet-based methods are better for low SNRs, less smoothing methods are better for moderate and high SNRs.

4.2 Effect on the shape of the detected spots

We also compared the temporal SNR maps of the denoised time series. Fig. 4 shows temporal SNR maps of the area containing the active spot. In the noise-free case, all points in the spot have the same temporal SNR. With heavy Gaussian smoothing, the detected spot becomes elliptic. Gaussian smoothing and smoothing wavelet-based methods, which perform well for low input SNRs, change the shape and the intensity distribution of the detected region. Less smoothing wavelet-based methods show smaller deformations. We segmented the images into an 'active' area and a 'non-active' area, using a histogram-based threshold. We computed the number of points labelled 'active' outside the original spot, and points labelled 'non-active' inside the original spot. Heavy Gaussian smoothing yielded many errors of the first type, and both Gaussian smoothing and smoothing wavelet-based methods showed more errors of the second type. This was due to deformations of the active spot. Especially the less smoothing wavelet denoising schemes keep the edges of the spot sharp. This difference may have serious consequences when statistical activity maps are built from denoised fMRI time series.

5 CONCLUSIONS

We have compared wavelet denoising and Gaussian smoothing in two settings: 2D images and time series of 2D images, both contaminated by white or $1/f$ noise. Smoothing wavelet methods are favourable when the SNR of the input image is relatively low, non-smoothing wavelet-based methods are better for images with a higher SNR. A disadvantage of Gaussian smoothing is the dramatic change of the shape of active regions and their distributions of SNR values. This effect is much less severe in wavelet-based denoising.

In future work, we will make statistical analyses of denoised fMRI data to test our denoising methods, with a focus on the shape of regions detected with statistical methods. We expect to find similar results in PET data, although the noise model and the expected SNR are different from those in fMRI. Another future direction is the use of temporal, as opposed to spatial, denoising of neuroimaging data.
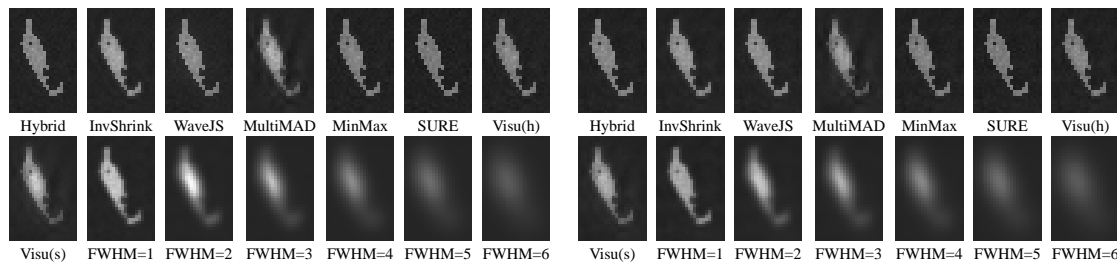
6 ACKNOWLEDGMENTS

Figure 4. Temporal SNR maps in the area around the active spot. The original images were perturbed by white noise (left) and $1/f$ noise (right) with a spatial SNR of 10 dB.

REFERENCES

[1] R. Turner, A. Howseman, G.E. Rees, O. Josephs, and K.J. Friston. Functional magnetic resonance imaging of the human brain: data acquisition and analysis. *Exp. Brain Res.*, 123:5–12, 1998.

[2] U.E. Ruttimann, M. Unser, R.R. Rawlings, D. Rio, N.F. Ramsey, V.S. Mattay, D.W. Hommer, J.A. Frank, and D.R. Weinberger. Statistical analysis of functional MRI data in the wavelet domain. *IEEE Trans. Med. Im.*, 17(2):142–154, 1998.

[3] J. Raz and B. Turetsky. Wavelet ANOVA and fMRI. In *Proc. SPIE*, volume 3813, pages 561–570, 1999.

[4] M. Hilton, T. Ogden, D. Hattery, G. Eden, and B. Jawerth. Wavelet processing of functional MRI data. In A. Aldroubi and M. Unser, editors, *Wavelets in Biology and Medicine*. CRC Press, 1996.

[5] J.B. Buckheit and D.L. Donoho. Wavelab and reproducible research. Technical Report 474, Dept. of statistics, Stanford University, 1995. http://www-stat.stanford.edu/~wavelab.

[6] S.G. Mallat. A theory for multiresolution signal decomposition: The wavelet representation. *IEEE Trans. PAMI*, 11(7):674–693, 1989.

[7] M. Unser. Splines: A perfect fit for signal and image processing. *IEEE Sign. Proc. Mag.*, 16(6):22–38, 1999.

[8] D.L. Donoho and I.M. Johnstone. Adapting to unknown smoothness by wavelet shrinkage. *J. Amer. Stat. Assoc.*, 90:1200–1224, 1995.

[9] D.L. Donoho and I.M. Johnstone. Ideal denoising in an orthonormal basis chosen from a library of bases. *Comp. Rend. Acad. Sc. A*, 319:1317–1322, 1994.